Vortex-Pair Dynamics in Anisotropic Bistable Media: A Kinematic Approach

Aric Hagberg[1] and Ehud Meron[2,3]

[1]*Mathematical Modeling and Analysis, Theoretical Division, Los Alamos National Laboratory,
Los Alamos, New Mexico 87545, USA*
[2]*Department of Solar Energy and Environmental Physics, BIDR, Ben Gurion University, Sede Boker Campus 84990, Israel*
[3]*Department of Physics, Ben-Gurion University, Beer Sheva, 84105, Israel*

In isotropic bistable media, a vortex pair typically evolves into rotating spiral waves. In an anisotropic system, instead of spiral waves, the vortices can form wave fragments that propagate with a constant speed in a given direction determined by the system's anisotropy. The fragments may propagate invariably, shrink, or expand. We develop a kinematic approach for the study of vortex-pair dynamics in anisotropic bistable media and use it to capture the wave fragment dynamics.

Spiral vortices are common spatiotemporal patterns in a variety of oscillatory, excitable, and bistable systems. Numerous studies have been devoted to their structure, stability, formation mechanisms, mutual interactions, and control techniques. In bistable media spiral vortices are closely related to the nonequilibrium Ising-Bloch (NIB) bifurcation, a pitchfork front bifurcation that renders a stationary "Ising" front unstable and leads to a pair of counterpropagating "Bloch" fronts. The NIB bifurcation has been observed in various systems, including liquid crystals [1] and chemical reactions [5,6], and has been the subject of many theoretical studies [4].

The NIB bifurcation designates the onset of traveling waves in general, and spiral waves in particular. A number of other pattern formation phenomena in isotropic bistable systems can be attributed to the NIB bifurcation. They include temporal events, such as when one Bloch front transforms into the other; this process changes the direction of front propagation. These transformations can be induced by an increase in front curvature, front interactions, and other disturbances. When the transformation takes place uniformly along the front line, it leads to phenomena such as reflection of fronts and breathing patterns [5]. When the transformation is local, it leads to the nucleation of spiral-vortex pairs [6].

Front reflection, breathing structures, and spiral-vortex nucleation may occur in anisotropic bistable media as well. The anisotropy of the system, however, may induce additional pattern formation phenomena not found in isotropic systems [7]. An intriguing example is traveling wave fragments observed in catalytic reduction of NO with hydrogen on a Rh(110) surface [8] and in catalytic oxidation of CO on Pt(110) [9]. These fragments travel at constant speeds in specific directions and, depending on parameters (e.g., hydrogen partial pressure in the NO reduction reaction), either shrink or expand. The phenomenon has been reproduced in simulations of a reaction-diffusion model representing an excitable medium with nonlinear anisotropic diffusion [8].

In this Letter we study vortex-pair dynamics in two-dimensional anisotropic bistable media and identify a general mechanism for traveling fragments. We show that traveling fragments develop when Bloch fronts in a given direction transform into Ising fronts in the orthogonal direction. The origin of the anisotropy appears irrelevant as long as it is capable of inducing the change of front type upon rotation by $\pi/2$.

We study vortex-pair dynamics by deriving kinematic equations for a front with contour lines that form a closed loop. Equations of this kind, but for isotropic systems and infinite front lines, have been derived in Ref. [6]. They consist of coupled integro-differential equations for the front curvature and front velocity where the independent variables are the arclength along the front line $s(t)$ and time t. We now extend these equations to fronts forming closed loops in anisotropic media using, as a case study, the FitzHugh-Nagumo model with diffusion anisotropy.

The anisotropic FitzHugh-Nagumo model is

$$\frac{\partial u}{\partial t} = \frac{1}{\epsilon}(u - u^3 - v) + \frac{1}{\delta}\left[\nabla^2 u + d\frac{\partial^2 u}{\partial y^2}\right],$$
$$\frac{\partial v}{\partial t} = u - a_1 v - a_0 + \nabla^2 v, \tag{1}$$

where u is the activator and v the inhibitor, and the anisotropy is quantified by the parameter d. The parameters a_0 and a_1 are chosen so that Eqs. (1) describe a bistable medium with two stable uniform states, (u_+, v_+) and (u_-, v_-). For $a_0 = 0$ the two uniform states are symmetric, $(u_+, v_+) = -(u_-, v_-)$. Ising and Bloch-front solutions connect these states as the spatial coordinate normal to the front goes from $-\infty$ to $+\infty$. For a symmetric system ($a_0 = 0$) the two Bloch fronts propagate at the same speed (but in opposite directions). We consider the sharp interface regime $\epsilon/\delta \ll 1$, in which the activator u varies steeply across a front while the inhibitor v varies smoothly. We further choose parameter values so that the isotropic system ($d = 0$) is near the NIB bifurcation [6], and the effect of switching d on and

rotating the angle θ by $\pi/2$ is to transform Ising fronts, propagating in the x direction, to Bloch fronts, propagating in the y direction.

We parametrize the front loop (identified with the $u = 0$ contour line) by the ratio, $\sigma(s) = s(t)/L(t)$, of the arclength with respect to the total loop length $L(t)$. We assume that this ratio is independent of time (this amounts to a proper choice of the tangential front velocity) [10]. The front loop dynamics is governed by the equation

$$\frac{d\mathbf{X}}{dt} = C_n \hat{r} + C_t \hat{s}, \qquad (2)$$

where $\mathbf{X}(\sigma, t)$ is the instantaneous position vector of the front, $\hat{r}(\sigma, t)$ and $\hat{s}(\sigma, t)$ are unit vectors perpendicular and tangent, respectively, to the front line, $C_n(\sigma, t)$ is the normal front velocity, and $C_t(\sigma, t)$ is the tangential front velocity. The normal front velocity is derived from the anisotropic FitzHugh-Nagumo model using singular perturbation theory in a parameter range where $\epsilon/\delta \ll 1$ [6]. It reads

$$C_n = \rho C_0 - (1 - \Delta)\kappa, \qquad (3)$$

where κ is the front curvature, $\Delta = 1 - (1 + d)/\delta\rho^2$, $\rho = \sqrt{(1 + d\cos^2\theta)}$, and θ is the angle between $\hat{s}$ and the x axis. Far from the NIB bifurcation C_0 is constant and represents the velocity of a planar front propagating in the y direction ($\theta = 0$). Near the NIB bifurcation C_0 becomes a slowly varying order parameter [6] satisfying Eq. (6) below. It is related to the value v_f of the inhibitor at the front position (where $u = 0$) via $C_0 = -3v_f/\eta\sqrt{2}$. The tangential front velocity (which does not have a physical meaning) is determined by the parametrization we chose for the front loop. It reads [10]

$$C_t = \sigma L \oint \kappa C_n d\sigma' - L \int_0^\sigma \kappa C_n d\sigma', \qquad (4)$$

where κ is the front curvature and the first integral in Eq. (4) is over the entire front loop ($0 \leq \sigma \leq 1$).

The instantaneous values of the front curvature κ and the order parameter C_0 along the front loop are determined by solving the following system:

$$\frac{\partial \kappa}{\partial t} = -\left(\kappa^2 + \frac{1}{L^2}\frac{\partial^2}{\partial\sigma^2}\right)C_n + \frac{1}{L}\frac{\partial\kappa}{\partial\sigma}C_t, \qquad (5)$$

$$\frac{\partial C_0}{\partial t} = (\alpha_c - \alpha)C_0 - \beta C_0^3 + \gamma\Delta\kappa + \gamma_0 + \frac{1}{L^2}\frac{\partial^2 C_0}{\partial\sigma^2}$$
$$+ \frac{1}{L}\frac{\partial C_0}{\partial\sigma}C_t, \qquad (6)$$

where $L(t)$, the total loop length, is determined by

$$\frac{\partial L}{\partial t} = L \oint \kappa C_n d\sigma', \qquad (7)$$

and the angle $\theta(\sigma, t)$ is related to the curvature via

$$\theta = -L\int_0^\sigma \kappa d\sigma'. \qquad (8)$$

In Eq. (6) $\alpha = \eta\sqrt{2}/\rho q\eta_c^2$, $\alpha_c = \sqrt{2}/q\eta_c$, $\beta = \eta^2/6\eta_c^2$, $\gamma = \sqrt{2}/\eta q$, $\gamma_0 = 2\sqrt{2}a_0/\eta$, $\eta = \sqrt{\epsilon\delta}$, $\eta_c = 3/2\sqrt{2}q^3$, and $q = \sqrt{a_1 + 1/2}$. Equation (5) for the curvature follows from pure geometrical considerations [11–13]. Equation (6) has been derived for the anisotropic FitzHugh-Nagumo model (using a singular perturbation analysis), but the form of this equation is general and expected to apply, apart from the angular dependence, to other anisotropic bistable systems that go through the NIB bifurcation.

According to Eq. (6) the threshold of the NIB bifurcation for a symmetric system ($a_0 = 0$) is given by $\alpha = \alpha_c$ or $\eta = \rho\eta_c$. The conditions for having Ising fronts propagating in the x direction ($\theta = \pi/2$) and Bloch fronts propagating in the y direction ($\theta = 0$) are

$$\eta_c < \eta < \eta_c\sqrt{1 + d}. \qquad (9)$$

The transformation from Ising front to Bloch fronts, as the angle θ is rotated from zero to $\pi/2$, is best illustrated by drawing velocity-curvature relations at various θ values. These relations are obtained from Eq. (6) by setting all derivatives to zero, solving for C_0 in terms of κ, and inserting the result in Eq. (3). Figure 1 shows such relations for d values satisfying Eq. (9). The solid lines refer to propagation in the y direction. They describe a pair of stable Bloch fronts and an unstable Ising front. The dashed line refers to propagation in the x direction and describe a stable Ising front. For the chosen symmetric condition, $\gamma_0 = 0$ (or $a_0 = 0$), the planar Ising front is
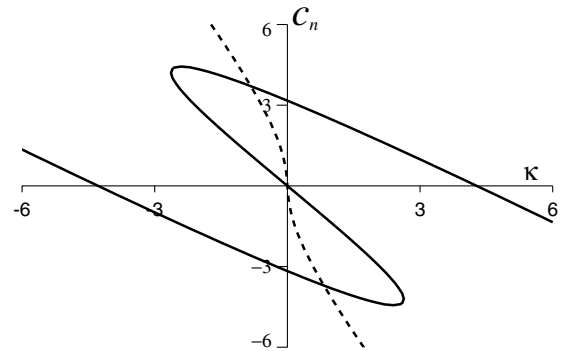

FIG. 1. Relationships between the normal velocity C_n and curvature κ in orthogonal directions that yields traveling wave fragments. The curves are obtained by setting all the derivatives to zero in Eq. (6), solving for C_0, and then using Eq. (3). The dashed curve is for fronts propagating in the x direction and indicates the existence of a single stable Ising front ($C = \kappa = 0$). The solid curve is for a front propagating in the y direction and indicates a pair of stable Bloch fronts ($C_n \approx \pm 3$, $\kappa = 0$). Parameters: $\epsilon = 0.07$, $\delta = 1.1$, $a_0 = 0$, $a_1 = 2$, $d = 1$.
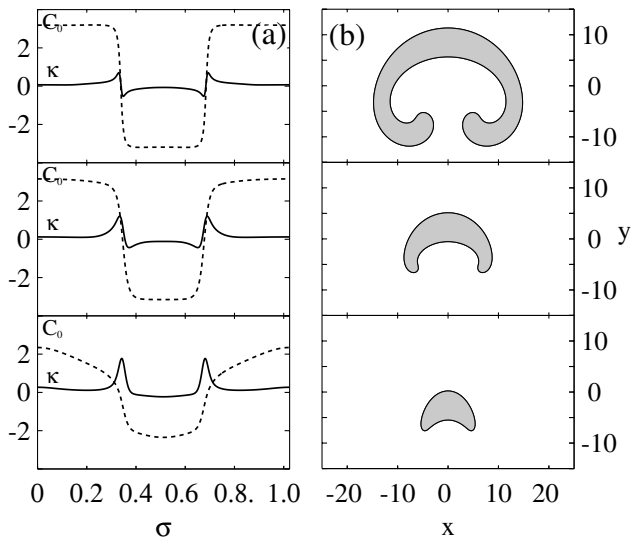
FIG. 2.   Formation of a pair of spiral waves in the Bloch regime of the isotropic case. (a) Solutions to the kinematic equations (5)–(7) at $t = 0$ (bottom), $t = 2$ (middle), and $t = 4$ (top). (b) The corresponding solutions in the $x - y$ plane. Parameters: $\epsilon = 0.035$, $\delta = 1.1$, $a_0 = 0$, $a_1 = 2$, $d = 0$.
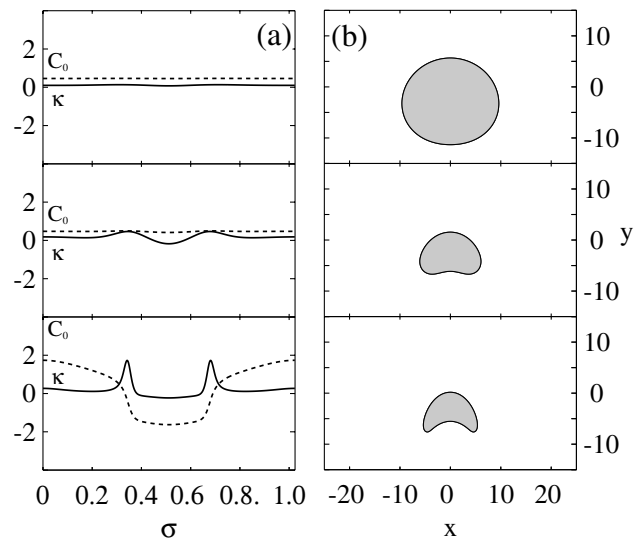

FIG. 3.   Formation of an expanding circular loop in the Ising regime of the isotropic case. (a) Solutions to the kinematic equations (5)–(7) at $t = 0$ (bottom), $t = 3$ (middle), and $t = 15$ (top). (b) The corresponding solutions in the $x - y$ plane. Parameters: $\epsilon = 0.14$, $\delta = 1.1$, $a_0 = 0.1$, $a_1 = 2$, $d = 0$.

stationary, but a positively curved Ising front propagates at a negative velocity. The negative slopes of the solid and dashed lines imply stability to transverse perturbations.

We recall [6] that the existence of counterpropagating Bloch fronts allows for traveling waves, in general, and spiral waves, in particular. A spiral-wave solution of the FitzHugh-Nagumo model (or any other reaction-diffusion system) corresponds to a front solution of the kinematic equations. Figure 2 shows the dynamics of a spiral-vortex pair in the isotropic case ($d = 0$). Solutions of the kinematic equations (5)–(7) are shown in Fig. 2(a), while the corresponding front curves in the physical $x - y$ plane, obtained from Eq. (2), are shown in Fig. 2(b). The vortex pair appears in Fig. 2(a) as a pair of fronts bounding a domain of one Bloch front surrounded by the other Bloch front. In the $x - y$ plane, the initial vortex pair forms a front loop that evolves into a pair of counter-rotating spiral waves.

Similar initial conditions in the isotropic case ($d = 0$), but for parameters corresponding to the Ising regime, lead to uniform velocity and curvature solutions of the kinematic equations as Fig. 3(a) shows. In the $x - y$ plane, these solutions describe the convergence to a shrinking circular loop or, for $a_0 > 0$ and not too small, to an expanding loop as Fig. 3(b) shows.

We now consider an anisotropic system with d satisfying Eq. (9) and a velocity-curvature relation for a symmetric system ($a_0 = \gamma_0 = 0$) as in Fig. 1. The Bloch fronts propagating in the y direction can form traveling waves, but no traveling waves can develop in the orthogonal x direction. As a result, and unlike the isotropic case, a vortex pair forming an initial loop as in Fig. 2(b) will not develop into a pair of counterrotating

spiral waves. It will instead form a traveling wave fragment propagating at constant speed without changing its shape as Fig. 4(b) shows. The corresponding solutions of the kinematic equations are shown in Fig. 4(a).

Breaking the symmetry between the two Bloch fronts in the y direction by choosing nonzero γ_0 (a_0)
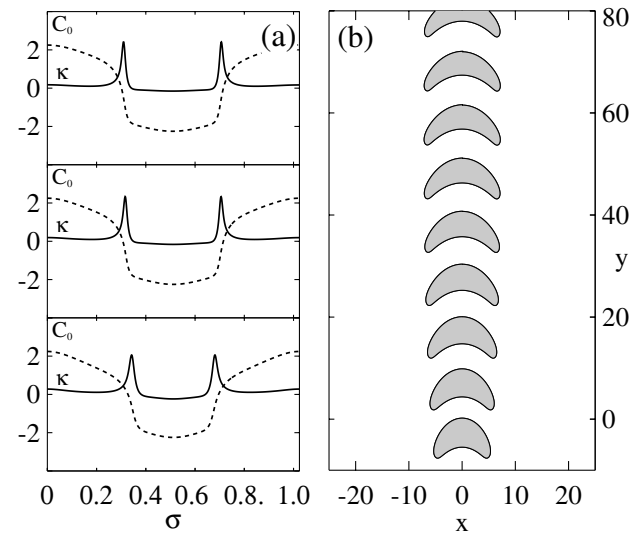

FIG. 4.   A traveling fragment in the symmetric ($a_0 = \gamma_0 = 0$) anisotropic case. For the symmetric case, the Bloch fronts that make up the front and back of the fragment travel with the same speed. (a) Numerical solutions to the kinematic equations (5)–(7) at $t = 0$ (bottom), $t = 25$ (middle), and $t = 50$ (top). (b) The fragment in the $x - y$ plane shown at different times on the same plot. The solutions are given for $t = 0$ to $t = 50$ in steps of $\Delta t = 5$. Parameters: $\epsilon = 0.07$, $\delta = 1.1$, $a_0 = 0$, $a_1 = 2$, $d = 1$.
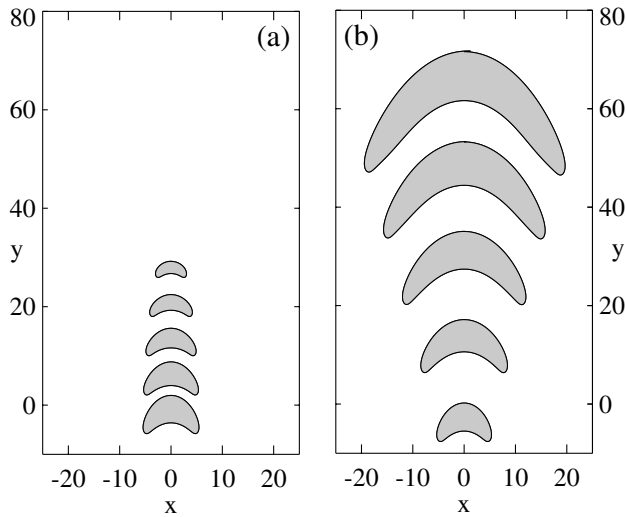
FIG. 5. Expanding and shrinking fragments obtained by solving the kinematic equations (5)–(7) numerically. (a) Shrinking fragment in the $x - y$ plane shown at different times on the same plot. The leading Bloch front is slower than the trailing Bloch front. The solutions are given for $t = 0$ to $t = 14$ in steps of $\Delta t = 3.5$. Parameters: $\epsilon = 0.07$, $\delta = 1.1$, $a_0 = -0.01$, $a_1 = 2$, $d = 1$. (b) Expanding fragment in the $x - y$ plane shown at different times on the same plot. The leading Bloch front is faster than the trailing Bloch front. The solutions are given for $t = 0$ to $t = 30$ in steps of $\Delta t = 7.5$. Parameters: $\epsilon = 0.07$, $\delta = 1.1$, $a_0 = 0.01$, $a_1 = 2$, $d = 1$.

values leads to traveling fragments that still propagate at constant speeds but either shrink ($\gamma_0 < 0$) or expand ($\gamma_0 > 0$), as Fig. 5 demonstrates. The edges of an expanding fragment trace straight lines and form a conelike shape. These results are in agreement with the qualitative experimental results reported in Ref. [9]. A fragment extends its length when the leading Bloch front propagates faster than the trailing one and reduces its length in the opposite case.

Traveling fragments may not appear only as solitary waves. The condition by which Bloch fronts transform to Ising fronts upon rotation by $\pi/2$ may also lead to "stratified chaos" [7], a dynamic state in which the disorder is confined to one direction (the direction of Bloch-front propagation). Traveling fragments ("blobs" in Ref. [7]) in this state repeatedly nucleate and annihilate and thereby nurture the chaotic dynamics. In this regard traveling fragments play a similar role to that of spiral vortices in isotropic media, whose spontaneous nucleation leads to spiral turbulence [14]. The unidirectional motion of the fragments preserves the stratified structure of the disordered pattern.

In this Letter we used a kinematic approach to study vortex-pair dynamics in anisotropic bistable media and proposed a general mechanism for traveling fragments. The advantage of the kinematic approach lies in the universal form of the kinematic equations near the NIB

bifurcation and, thus, in the generic nature of the results this approach yields.

[1] K. B. Migler and R. B. Meyer, Physica (Amsterdam) **71D**, 412 (1994); T. Frisch, S. Rica, P. Coullet, and J. M. Gilli, Phys. Rev. Lett. **72**, 1471 (1994); S. Nasuno, N. Yoshimo, and S. Kai, Phys. Rev. E **51**, 1598 (1995); T. Frisch and J. M. Gilli, J. Phys. II (France) **5**, 561 (1995).

[2] G. Haas, M. Bär, I. G. Kevrekidis, P. B. Rasmussen, H. H. Rotermund, and G. Ertl, Phys. Rev. Lett. **75**, 3560 (1995).

[3] K. J. Lee and H. L. Swinney, Phys. Rev. E **51**, 1899 (1995); G. Li, Q. Ouyang, and H. L. Swinney, J. Chem. Phys. **105**, 10 830 (1996).

[4] H. Ikeda, M. Mimura, and Y. Nishiura, Nonlinear Anal. Theory Methods Appl. **13**, 507 (1989); P. Coullet, J. Lega, B. Houchmanzadeh, and J. Lajzerowicz, Phys. Rev. Lett. **65**, 1352 (1990); A. Hagberg and E. Meron, Nonlinearity **7**, 805 (1994); M. Bode, A. Reuter, R. Schmeling, and H.-G. Purwins, Phys. Lett. A **185**, 70 (1994); E. P. Zemskov, V. S. Zykov, K. Kassner, and S. C. Müller, Nonlinearity **13**, 2063 (2000); D. Michaelis, U. Peschel, F. Lederer, D.V. Skryabin, and W. J. Firth, Phys. Rev. E **63**, 066602 (2001); D.V. Skryabin, A. Yulin, D. Michaelis, W. J. Firth, G.-L. Oppo, U. Peschel, and F. Lederer, Phys. Rev. E **64**, 056618 (2001).

[5] D. Haim, G. Li, Q. Ouyang, W. D. McCormick, H. L. Swinney, A. Hagberg, and E. Meron, Phys. Rev. Lett. **77**, 190 (1996); E. P. Zemskov, V. S. Zykov, K. Kassner, and S. C. Müller, Physica (Amsterdam) **183D**, 117 (2003); C. Hemming and R. Kapral, Physica (Amsterdam) **306A**, 199 (2002).

[6] A. Hagberg and E. Meron, Phys. Rev. Lett. **78**, 1166 (1997); Physica (Amsterdam) **123D**, 460 (1998); Physica (Amsterdam) **249A**, 118 (1998).

[7] M. Bär, A. Hagberg, E. Meron, and U. Thiele, Phys. Rev. Lett. **83**, 2664 (1999); Phys. Rev. E **62**, 366 (2000).

[8] F. Mertens, N. Gottschalk, M. Bär, M. Eiswirth, A. Mikhailov, and R. Imbihl, Phys. Rev. E **51**, R5193 (1995).

[9] H. H. Rotermund, S. Jakubith, A. von Oertzen, and G. Ertl, Phys. Rev. Lett. **66**, 3083 (1991).

[10] Z. Csahok, C. Misbah, and A. Valance, Physica (Amsterdam) **128D**, 87 (1999).

[11] R. C. Brower, D. A. Kessler, J. Koplik, and H. Levine, Phys. Rev. A **29**, 1335 (1984).

[12] E. Meron and P. Pelcé, Phys. Rev. Lett. **60**, 1880 (1988).

[13] A. S. Mikhailov, *Foundation of Synergetics I: Distributed Active Systems* (Springer-Verlag, Berlin, 1990).

[14] A. Hagberg and E. Meron, Phys. Rev. Lett. **72**, 2494 (1994); Chaos **4**, 477 (1994).